Ocean & Sea Ice SAF

Associated & Visiting Scientist Activity Report

Validation and Comparison of OSI SAF Low and Medium Resolution and IFREMER/Cersat Sea ice drift products

(Phil) Byongjun Hwang
Thomas Lavergne

The EUMETSAT
Network of
Satellite Application
Facilities

OSI SAF
Ocean and Sea Ice

SCOTTISH
ASSOCIATION
for MARINE
SCIENCE

Documentation Change Record

Version	Date	Author	Description
V0.0	04/29/10	PH	first draft
V0.1	05/05/10	PH,TL	Review and correction by TL
V1.0	05/27/10	PH,TL	Minor correction by GD
V1.1	10/09/10	TL	Implement comments from Fanny Ardhuin
V1.2	13/09/10	PH	Minor correction by PH

CONTENTS

1. Introduction

1.1 Overview

OSI SAF Low Resolution Sea Ice Drift (OSI-405) and Medium Resolution Sea Ice Drift (OSI-407) products were introduced as a result of the first Continuous Development and Operations Phase [CDOP, 2007 to 2012]. After sucessful development of these products under joint met.no and DMI responsibility (hereafter Project Team), the Operational Readiness Review (ORR) for OSI-405 (October 2009) concluded in the need for extending the validation exercise of these products in order to:

• conduct an inter-comparison with the products of IFREMER/Cersat (hereafter IFR),
• gain confidence in the error statistics of the single-sensor OSI-405 datasets (from AMSR-E, ASCAT and SSM/I) as a step towards the multi-sensor OSI-405 dataset.

Both the cited ORR and an earlier Product Consolidation Review (PCR) suggested to setup a Associated & Visiting Scientist Activity (AVSA) for tackling some of the two aspects. A proposal for AVSA, submitted in Janaury 2010, has been approved mid-Februray 2010. In the proposal, two reports were identified - the first one focusing on inter-comparison with IFR products and the second one focusing on 3-way comparison of OSI-405 single sensor products.

For the first report, it has been suggested that direct inter-comparison between OSI-405 and IFR products is not suitable since they do not share the same spatial and temporal characteristics, but rather indirect comparison, e.g. each product validates against in-situ GPS trajecatories, is more appropriate. It has also been suggested to include OSI-407 in the validation exercise.

At the kick-off meeting held on 11 March 2010 at met.no, both Project Team and VS realised total 8 weeks of project period is very time-pressing and agreed to limit our efforts to ITP trajectories as validation datasets (with possbility to include more in situ validation datasets in the future activity). We also agreed in the need for a sensitivity study to check the variability in error statistics with different collocation constraints.

This first report contains the results of the sensitivity study and validation of both OSI SAF and IFR products and a discussion of validation results. The report also provides statistics, graphs, and information about collocation procedure and software used.

1.2 Glossary

AMSR-E	Advanced Microwave Scanning Radiometer for EOS
ASAR	Advanced Synthetic Aperture Radar
ASCAT	Advanced SCATterometer
AVHRR	Advanced Very High Resolution Radiometer
CERSAT	Center for Satellite Exploitation and Research
CDOP	Continuous Development and Operations Phase
CMCC	Continuous Maximum Cross Correlation

DMI	Danish Meteorological Institute
DTU	Technical University of Denmark
GCTP	General Cartographic Transformation Package
GPS	Global Positioning System
IFREMER	French Research Institute for Exploitation of the Sea
ITP	Ice Tethered Profiler
NSIDC	National Snow and Ice Data Center
MCC	Maximum Cross Correlation
met.no	Norwegian Meteorological Institute
OSI SAF	Ocean and Sea Ice Satellite Application Facility
QuikSCAT	Quick SCATterometer onboard Seawinds satellite
SSM/I	Special Sensor Microwave/Imager

2. Sea ice drift products and validation dataset

2.1 Sea ice drift products

In this report, we targeted six sea ice drift products to be validated against in situ GPS trajectories (Table 1). OSI-405 and 407 product datasets were obtained directly from Project Team at the kick-off meeting. IFR product data were downloaded from IFREMER ftp site [1].

OSI-405 (low resolution) ice drift are computed on a daily basis from aggregated maps of passive microwave (e.g. SSM/I, AMSR-E) or scatterometer (e.g. ASCAT) data. OSI-405 AMSR product uses 37 GHz, H and V polarisations [2]. OSI-405 Multi product is produced by merging SSM/I (85 GHz), AMSR-E (37 GHz) and ASCAT (σ°) single-sensor ice drift products. IFR-Merged ice drift are derived by merging SSM/I (85 GHz) and QuikSCAT (σ°) ice drift products, themselves obtained from aggregated satellite images with typical resolution of 12.5 km x 12.5 km [4], and IFR-89GHz from AMSR-E (89 GHz) daily images with a resolution of 6.25 km x 6.25 km [3]. OSI-407 ice drift are computed from AVHRR band 2 (visible) & 4 (infrared) swath images with a resolution of 1.1 km [5].

Product	Source	Source Data	Grid Spacing	Time Span	Area Averaging
OSI-405 AMSR	OSI SAF	AMSR-E 37 GHz H/V	62.5 km	48 hrs	~140x140 km^2
OSI-405 Multi	OSI SAF	SSM/I, AMSR-E, ASCAT	62.5 km	48 hrs	~140x140 km^2
IFR-Merged (not filled)	IFREMER/ Cersat	SSM/I, QuikSCAT	62.5 km	72 hrs	~140x140 km^2
IFR-89GHz	IFREMER/ Cersat	AMSR-E 89 GHz H/V	31.25 km	48 hrs	~70x70 km^2
OSI-407 VIS	OSI SAF	AVHRR band 2	20 km	24 hrs	~40x40 km^2
OSI-407 IR	OSI SAF	AVHRR band 4	20 km	24 hrs	~40x40 km^2

Table 1: Spatial and temporal characteristics for the sea ice drift products used in this report.

Area averaging is the area covered by the sub-images used in computing the cross-correlation metric and, thus, the motion vector. Ice drift products indeed do not contain the motion vector of a single point but instead the average motion over a rather large area of sea ice. From the pool of products we have been using, the OSI-407 products (from AVHRR imagery) have the smallest area averaging (40x40 km^2). The OSI-405 and IFR-Merged products have similar area averaging values although the shape of the area is different: the OSI-405 products adopt a quasi-circular shape while the IFR products use square shape. The image block for both the OSI-405 and IFR-Merged products are contained into a 11x11 pixels square shape, each image pixel being 12.5 km.

The differences between OSI-405 and IFR-Merged products lie in a) tracking algorithm and b) time interval. OSI-405 products adopt Continuous Maximum Cross Correlation (CMCC) method [2], where pixel values in the sub-images are interpolated from those in the nominal pixels. This is a more advanced method than the classical Maximum Cross Correlation

(MCC) which is used in IFR product as well as OSI-407 product [3,5]. The main advantage of CMCC method is in minimizing the quantification effects which is significant in low resolution products [6,11].

2.2 Validation data set

2.2.1 Ice Tethered Profilers

The Ice Tethered Profilers (ITP) platforms are advanced autonomous drifting instrument that are designed to measure temperature and salinity profiles in the ocean under sea ice. As part of its daily data stream, each ITP transfers hourly unfiltered GPS locations. During the validation period, a total of 37 ITPs are available (both active and completed missions). The data density of ITPs are much less than Argos-based buoys, but it is benefited from much more accurate GPS location of the trajectories.

The Ice-Tethered Profiler data were collected and made available by the Ice-Tethered Profiler Program based at the Woods Hole Oceanographic Institution (http://www.whoi.edu/itp).

3. Validation methodology

3.1 Validation variables and period

The primary variables are the X and Y displacement components in the product grid, namely dX and dY. The selection of dX and dY is based on the fact that these variables tend to less biased than vector direction and magnitude [10]. The collocation period spans three winter periods for low resolution products, but OSI-407 products were available for only the limited period of time (Table 2).

Product	Collocation period	Time constraint (hour)	Radius constraint (km)
OSI-405 AMSR	10/2006 to 04/2007 10/2007 to 04/2008 10/2008 to 04/2009	1, 2, and 3	20, 40, 60, 80, and 100
OSI-405 Multi		1, 2, and 3	20, 40, 60, 80, and 100
IFR-Merged		1, 2, and 3	20, 40, 60, 80, and 100
IFR-AMSR89		1, 2, and 3	10, 20, 30, 50, and 80
OSI-407 VIS	09/2008 to 07/2009	1	5, 10, 20, 30, and 40
OSI-407 IR	03/2009 to 10/2009	1	5, 10, 20, 30, and 40

Table 2 Time and radius constraints applied in the collocation process. The collocation was made for each combination of time and radius constraints, e.g. 1 hour and 20 km for OSI-405 AMSR.

3.2 Collocation strategies

The six sea ice drift products were all processed in the same Polar Stereographic projection, identical to the one used by NSIDC (i.e. true north=70N, center lat=45W, earth radius=6378.273 km and an eccentricity of 0.081816153). This ensures the dX and dY values in the six products share the same grid system.

All sea ice drift products contain time information at the starting point (t0) and end point (t1) of the ice drift vector. OSI-405 products come with the two types of time information: standard daily 1200 UTC and more accurate time for each vector, while IFR ice drift products only provide standard daily 1200 UTC. For consistency, a so called 2D collocation was chosen for both OSI-405 and IFR products. This means the time was set to be t0 = t1 = 1200 UTC everywhere in the product grid.

OSI-407 products record the time stamp for each swath. Though OSI-407 products has 24h time lag, the actual period of ice drift correspond to the time between the two swath data acquisitions. Thus the swath time was used for each vector grid for the collocation purpose (i.e. 3D collocation).

Regardless 2D or 3D collection, collocation was made to meet the three conditions:

– the time difference at the starting point (t0) between product and reference (ITP) should be smaller than the prescribed time constraints, e.g. |prd_t0 – ref_t0| < 1, 2, or 3 hours

– the distance (i.e. great circle distance[1]) at the starting point (t0) between product and reference (ITP) should be smaller than the prescribed radius constraints, e.g. dist(prd_xy_t0 – ref_xy_t0) < 20, 30, or 40 km, and

– the time difference at the end point (t1) between product and reference should be smaller than the same time constraint used at the starting point (t0) (e.g. |prd_t1 – ref_t1| < 1 hour).

For each product grid, there can be more than one matching reference points that meet the three collocation criteria above. The nearest-neighboring point in time (and space) was then selected among these points. This resulted in a single reference point of each ITP trajectory for each product grid point.

As for sensitivity study, different time and radius constraints were applied (Table 2). Radius constraints were selected in such a way that they encompass the area-averaging radius used by the ice drift tracking algorithm, e.g. the range of radius constraints from 20 km to 100 km for OSI-405 and IFR-Merged products well spans the area-averaging radius of 70 km (Table 1). Time constraints were set up for 1 to 3 hours to find any fluctuation in error statistics due to the relaxation of time constraints.

3.3 Graphs and statistics

3.3.1 Sensitivity plots
Sensitivity plots aim to describe the variability of error statistics (e.g. σ [dX],σ [dY]) according to time and radius constraints. Key point of the plots is to see any divergence or convergence of error statistics, in order to find the right set of constraints in further validation exercise.

3.3.2 2D histogram of dX and dY & scatter plot of reference vs. product
2D histogram plot is the same type of graph used in the report by Project Team [7]. It describes the sample distribution of the collocated points overlaid with ideal Gaussian (or Normal) distribution at 68% (1.5σ) and 95% (2.5σ) probability density based on the sample mean and standard deviations. The more the sample histogram become like-Gaussian, the more justify the implication of a Gaussian model commonly used in most assimilation methods.

Scatter plot is a common approach in error analysis. Note that the plot include both dX and dY components (so N become double), and the statistics in the plot are based on that.

3.3.3 Validation statistics
• the statistical bias in dX and dY: δ [dX] and δ [dY]
• the statistical standard deviation of the errors in both components: σ [dX] and σ [dY]
• the statistical correlation between the errors in both components: ρ [dX,dY]
• slope and intercept of a linear regression of product vs. reference: α , β
• correlation coefficient of product vs. reference: ρ

---

1 The shortest distance between two points on the surface of a sphere measured along a path on the surface of the sphere

4. The results of validation

4.1 Sensitivity study

The purpose of this sensitivity study are a) to check the variability of error statistics with various collocation constraints, and b) to help to justify the set of collocation constraints selected for the analysis in the following sections.

Effects of time constraints: Very little variability with different time constraints was found in N, σ[dX] and σ[dY] (Fig. 1). For example in the OSI-405 AMSR 40-km radius constraint case, from 1-hour to 3-hour time constraint only 45 number counts is added while σ[dX] and σ[dY] remain almost the same. This indicates the time constraints are not an important factor at least in our case, and gives us confidence to select just one of the three time constraints in the following validation sections. However we should note that the ITP trajectories used in this report are hourly, and the change of time constraints can be significant if in situ trajectories have random or longer time intervals between the position records.

Effects of radius constraints: Some variability with different radius constraints was found in N, σ[dX] and σ[dY] (Fig. 1). For low resolution products (OSI-405 and IFR), N jumped at the 40-km radius constraint and remained relatively stable afterward (Fig. 1a). For instance, N for OSI-405 AMSR was 1,329 at the 20-km radius constraint and then jumped to 4,572 at 40-km radius constraint. Note these numbers are comparable to the one (3,977) reported by Project Team [8]. Note that Project Team [8] used more validation data sources in addition to ITP data (not including GTS buoys (Argos positioning system)) but used the 30-km radius constraint.   Note also that both merged products (OSI-405 Multi and IFR-Merged) have higher number counts than single sensor ones. This demonstrates the advantage of merged products of having higher drift data density than the single sensor ones.

For OSI-407 VIS and IR products number counts (N) of collocated points are very small, e.g. only 12 to 63 and 50 to 583 for 5 km to 40 km radius constraint, respectively. These numbers are quite small compared to number counts in the report by Project Team where the GTS buoys (Argos positioning system) were used as validation data sets instead [9]. Most of those buoys reporting through GTS are from the International Arctic Buoy Program (IABP). In that report [9] 11,494 matching points for OSI-407 IR product were found during 09/2008 to 07/2009, and 2,217 matching points for OSI-407 VIS product during 03/2009 to 10/2009. Note we have longer validation periods than the previous report and that we only use the nearest-neighbor, while Project Team used all collocation points inside a given radius of 50 km [9]. Thus the relatively small N of ours is likely due to both the limited number of ITP trajectories (only 37) compared to IABP buoys and to different collocation strategies. However, note that Argos positioning system is much less accurate than GPS system used in ITP data.

There is a general tendency of increase in standard errors with increasing radius constraint (Fig. 1b and c), but difference exists among the products. In OSI-405 AMSR and IFR-Merged product, both σ[dX] and σ[dY] showed a steady, moderate increase with the radius constraint (about 0.5 km increase from 20 km to 40 km).   However, OSI-405 Multi and IFR-89GHz products show a jump in σ[dY] (Fig. 1c). The jump seems to be associated with the area-averaging radius of the products, but there is no clear explanation for why some products has a jump and others not. The error trends of OSI-407 products show very little variability between 10-km to 40-km radius constraints (Fig. 1b and c).
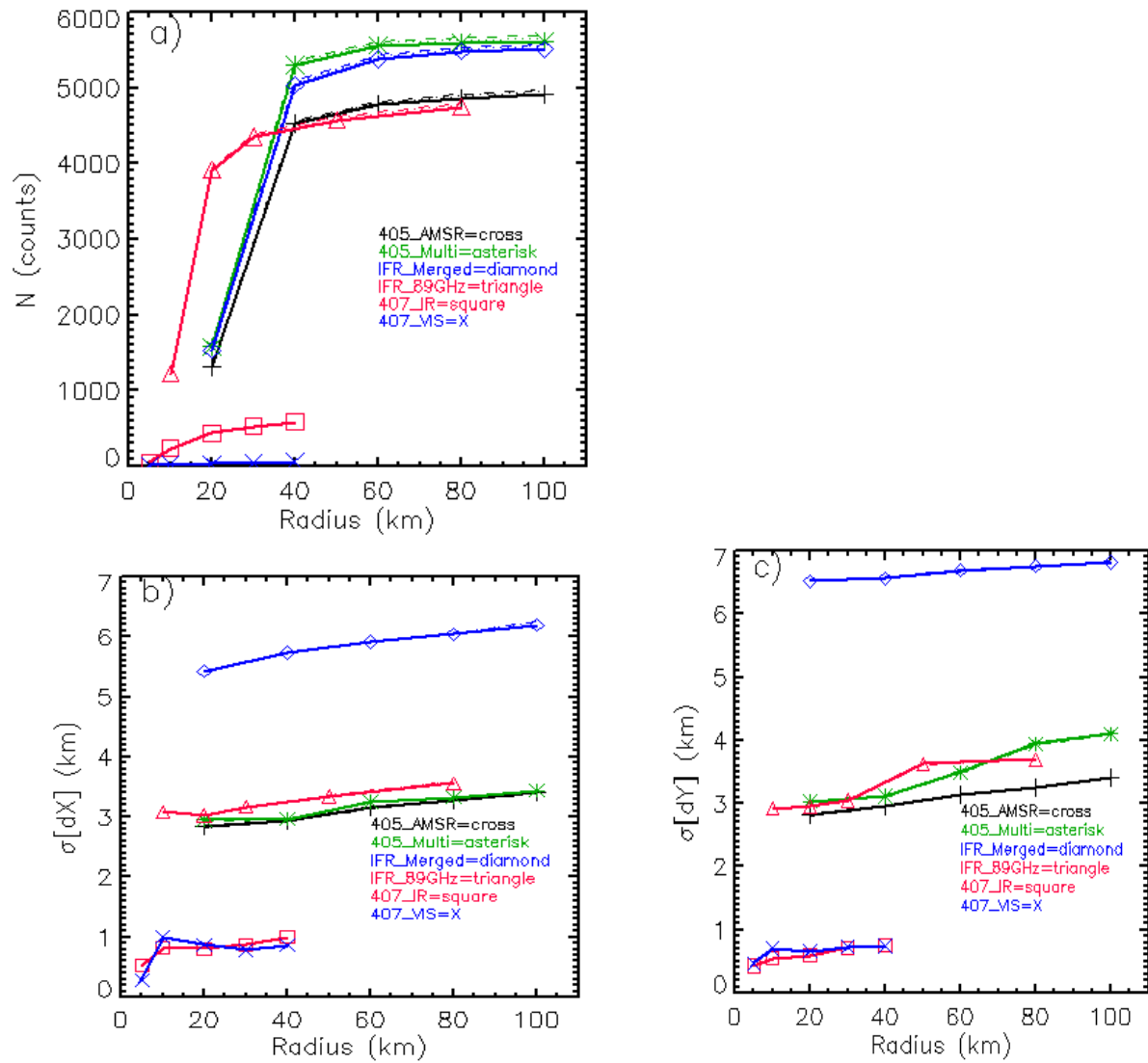
Figure 1 a) Number counts (N) of the collocated pairs and the standard deviations (σ[dX] and σ[dY]) of b) dX and c) dY versus radius constraints. Different colors and symbols indicate different ice drift products. Solid line with symbols indicate the collocation results for 1 hr time constraint, and dashed and dotted lines without symbols for 2 hr and 3 hr time constraints, respectively.

Based on these results, in the following validation sections we select only the collocation data set with the time constraints within 1 hour and the radius constraint for each product as follows;

• OSI-405 AMSR & Multi and IFR-Merged: 40 km,

• IFR-89GHz: 30 km, and

• OSI-407 IR & VIS: 40 km.

The radius of 40 km for OSI-405 and IFR-Merged products is selected as larger radius do not allow collecting much more collocation pairs (Figure 1a). Furthermore, the validation statistics are rather stable for larger collocation radiuses. It is true there is an increase in σ[dY] after 60-km radius constraint in OSI-405 Multi product. As it is beyond the area-averaging radius, We felt 40-km radius constraint is a more reasonable choice. The radius constraint of 30 km for IFR-89GHz product is selected as N become more stable at 30 km. There is an increase in σ[dY] after 50-km radius but they are beyond the area-averaging radius for that product. The radius constraint of 40 km for OSI-407 products is beyond the area-averaging radius of the products, but it is selected to have maximum number counts as we have very small number counts for the products. Note also the standard errors remain quite stable even beyond the searching radius.

The sensitivity study reported upon in this section ensures that the selected collocation radiuses allow:

1. large enough number of collocation pairs

2. that the reference drift vector is inside the area-averaging region (except for OSI-407)

3. that the conclusions we report in the next section are not depending on the collocation criteria we use.

4.2 Validation results of low resolution products

For OSI-405 AMSR, both σ[dX] and σ[dY] remain about 3.0 km, and 2D histogram of the sample is fairly close to the Gaussian distribution (Figure 2). These values are slightly lower than the ones (3.11 km and 3.05 km) reported in the validation report by Project Team [7]. This slight different values is due to different collocation constraints as well as the validation data sets used in that report, where other data sources were used in addition to ITP. The degree of un-correlation between dX and dY is also almost the same as reported in [7].

OSI-405 Multi product shows slightly higher σ[dX] and σ[dY] and slight lower α, compared to OSI-405 AMSR ones, while correlation (ρ) remains the same (Figure 2). Again, these values (2.96 km and 3.12 km) are lower than the ones (σ[dX]=3.65 km and σ[dY]=4.05 km) reported in [7]. In fact, the differences become larger in OSI-405 Multi compared to OSI-405 AMSR.

Note that OSI-405 AMSR and Multi share the same product grid and time interval (Table 1). A careful look at the scatter plot of OSI-405 Multi shows a general tendency of underestimation of product drifts relative to ITP ones (Figure 2). The cause of this is mainly due to merging of less accurate drift vectors from other products (i.e. SSM/I and ASCAT). In fact, there is a general tendency of increase in error in SSM/I and ASCAT products (see Table 2 in [7]).

IFR-Merged product has shown the largest error statistics against ITP trajectories among the low resolution products. σ[dX] and σ[dY] of this product are about 5.7 km to 6.6 km.. The 2D histogram shows more not-like Gaussian distribution than other products, dX and dY become

more correlated, and the underestimation of the product drifts become more evident in the scatter plot (Figure 3). This underestimation is probably related to the use of the Maximum Cross Correlation (MCC) method, by which all the drift components that are smaller than half a pixel are retrieved as 0 (quantization noise). In IFR-Merged product User's Manual ([4]), the standard deviation of the difference in vector magnitude between products and validation buoys is reported as 7.5 km. Although it remains cautious to compare statistics obtained with different collocation methods, against different validation datasets and for different time periods, it is comforting that the value reported in [4] is comparable to the one we find for IFR-Merged in the present study (7.2 km, not shown).

In the scatter plot of IFR-Merged product (Figure 3), the step-like feature indicates the quantification effects due to the pixel size δ of SSM/I and QuikSCAT maps (i.e. 12.5 km) [6]. In variance, this quantification effect accounts for $\delta^2/6$ for the module (5.1 km in standard deviation) and $\delta^2/12$ (3.6 km in standard deviation) for the components of the vector. Thus, σ[dX] (and σ[dY]) of remaining noise level are only 2.1 km and 3.0 km, which means the quantification effects accounts for more than half of the error statistics for IFR-Merged product.

IFR-89GHz product has shown the σ[dX] and σ[dY] values quite comparable with OSI-405's ones (Figure 3). The 2D histogram also shows more Gaussian-like distribution (Figure 3). The quantification effects can also be observed in the scatter plot, and is estimated to be 1.8 km in standard deviation of the error in dX and dY. This means the quantification effects account for about 60% of σ[dX] and σ[dY].

4.3   Validation results of medium resolution products

For Medium resolution product (i.e. OSI-407), we report only the scatter plots due to small number of collocation samples. These products clearly show small σ[dX] and σ[dY], and a good correlation (Figure 4). In fact, the σ[dX] and σ[dY] values are much lower (less than 1 km) than the ones of low resolution products. These values are slightly lower than the ones (1.35 km and 1.36 km) reported by Project Team [9]. The difference can be attributed to different validation data sets, e.g. Dybkjaer [9] used Argos positioning buoys, not ITP GPS data.

4.4   Inter-comparison

Although we implemented the same collocation strategy, against the same validation dataset and during the same time period, we cannot draw robust conclusion as far as the selection of a more or less accurate ice drift product is concerned. This is because the difference in time-span (1, 2 and 3 days) between the ice drift products under study does not allow for inter-comparing validation statistics that scale with the length of the drift vectors, as is the case for σ [dX] and σ [dY]. The 3-day product IFR-Merged is bound to have larger σ [dX] and σ [dY] compared to, e.g. OSI-405 MULTI, because the first one measures a 3-day drift, which will be longer (both in module and variability) than the 2-day drift measured by the OSI SAF products. Both OSI-405 and IFR-89GHz sample 2-day drifts and can be compared. OSI-407 samples 24-hour drift vectors and thus cannot be compared to any of the other drift products.

This being said, the correlation coefficient ρ can to some extent be compared among the six sea ice drift products. This is because ρ includes the first order (linear) portion of the scaling from 1-day to 3-day drifts, since ρ (u,v) does not depend on the linear transformation of the samples u and v. As far as this statistics is concerned, OSI-407 products show the highest

value (0.98) against ITP trajectories, followed by OSI-405 and IFR-89GHz (0.96), and the smallest for IFR-Merged (0.92) (Table 3). All 6 products show correlation of more than 0.9 against the validation dataset, which is very good.

OSI-405 and IFR-89GHz are both 2-day drift products (Table 1) and the validation results reported are very similar (Table 3), although slightly better for the OSI-405 products. The small differences in error statistics are related to the different spatial resolution, data source, and quantization effects. Note that IFR-89GHz benefits from higher spatial resolution than OSI-405 ones (6.25x6.25 km^2 against 12.5x12.5 km^2). Access to better resolution is however hampered by increasing atmospheric contamination at 89GHz, which might lead to more missing vectors in the IFR-89GHz product grid, especially in autumn and spring [4, Figure 8]. The quantization effect, which is clearly visible in Figure 3, has less strong effects on the validation statistics of IFR-89GHz. Thanks to the CMCC, the OSI-405 products are not plagued with the quantization noise (Figure 2) and achieve slightly better validation statistics, yet using lower resolution images.

As noted earlier, the module and natural variability in ice motion becomes larger with increasing time interval. For example, the standard deviation of X component of ITP trajectories (i.e. σ [dX_ref]) is about 4 km for OSI-407 time interval (1-day). This increases to about 11 km for two-day period (both OSI-405 products and IFR-89GHz) and 14.5 km for 3-day motion (IFR-Merged).

Figure 5 is an attempt to compare the standard deviation of the error (σ [dX]) to the natural variability of the 1-, 2-, or 3-day drift as measured by the ITP (σ [dX_ref]). Specifically, the OSI-407 statistics are normalized by the variability of 1-day drift vectors, the OSI-405 and IFR-89GHz by the variability of 2-day drift vectors and IFR-Merged by the variability of 3-day drift vectors. Intuitively, it is best to have small relative difference (σ [dX]/σ [dX_ref]) so that the natural variability in the ice displacement is captured by the satellite product. First, it should be noted that all products achieve values of σ [dX]/σ [dX_ref] less than 1. This confirms that, on average, all products resolve the natural variability over the associated drift period.

Product	N	δ[dX]	δ[dY]	σ[dX]	σ[dY]	ρ[dX,dY]	α	β	ρ
OSI-405 AMSR	4527	-0.04	-0.06	**2.93**	**2.95**	-0.04	0.95	-0.01	**0.96**
OSI-405 Multi	5303	-0.03	-0.11	**2.96**	**3.12**	-0.03	0.92	0.02	**0.96**
IFR-Merged	5040	0.09	-0.48	**5.74**	**6.57**	0.11	0.90	-0.04	**0.92**
IFR-AMSR89	4353	-0.03	-0.13	**3.17**	**3.05**	0.07	0.96	-0.04	**0.96**
OSI-407 VIS	583	-0.08	0.04	**1.00**	**0.75**	0.10	0.98	-0.02	**0.98**
OSI-407 IR	63	0.12	0.04	**0.87**	**0.74**	0.46	1.04	0.09	**0.98**

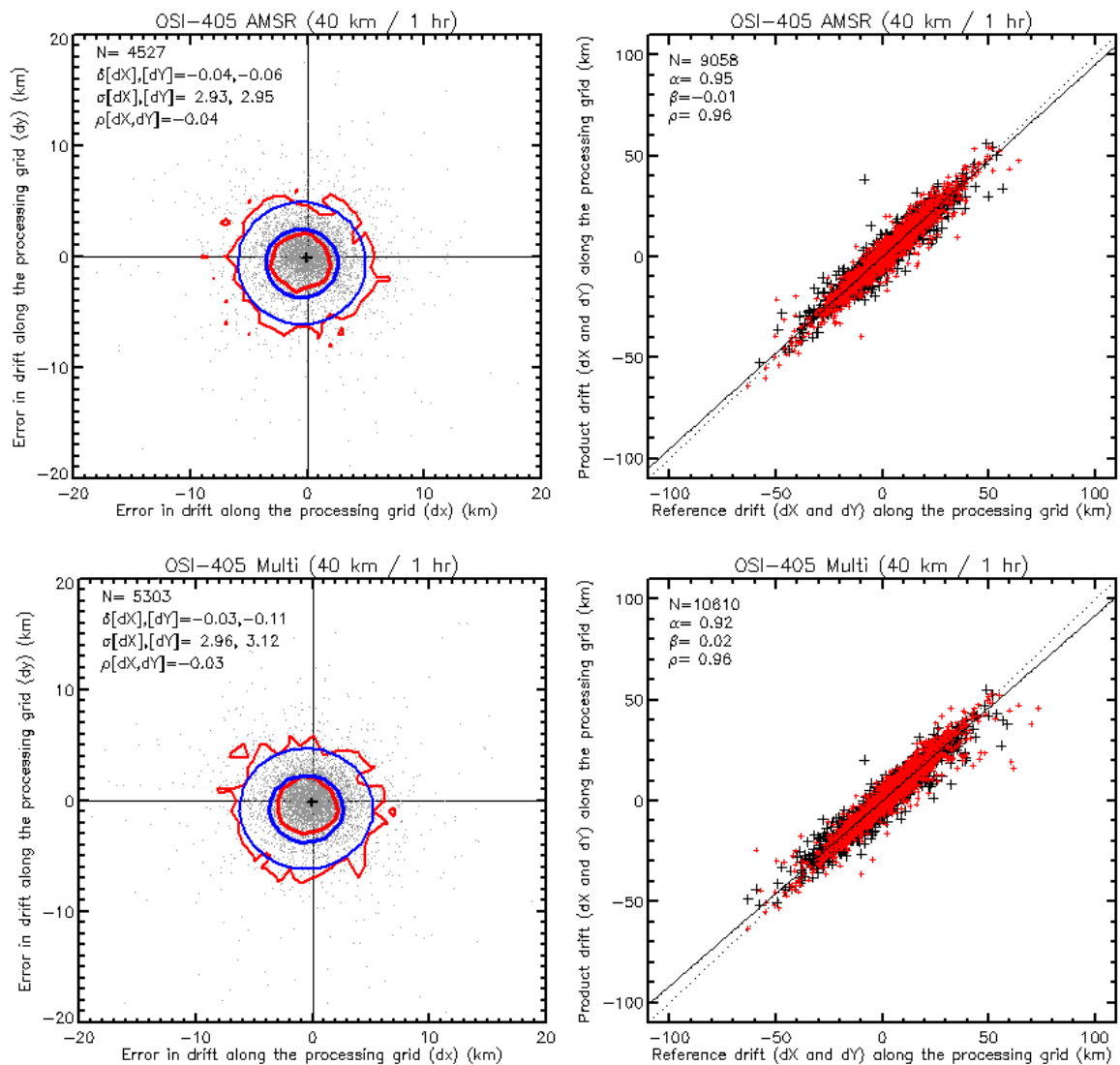Table 3. The error statistics of selected sea ice drift products.

Fig. 2. (left) 2D histogram plot along dX versus dY, and (right) scatter plot of product versus reference dX (black) and dY (red) for two OSI-405 products. In 2D histogram plots, red irregular contour line indicates the probability density at 68% (thick) and 95% (thin) of the sample, and blue circular contour line for the corresponding Normal distribution. The thick cross at the center indicate the bias of dX and dY. In the scatter plot, α and β are slope and intercept of linear regression (solid line), and ρ is the correlation coefficient. N is the total number counts of the validation pairs.
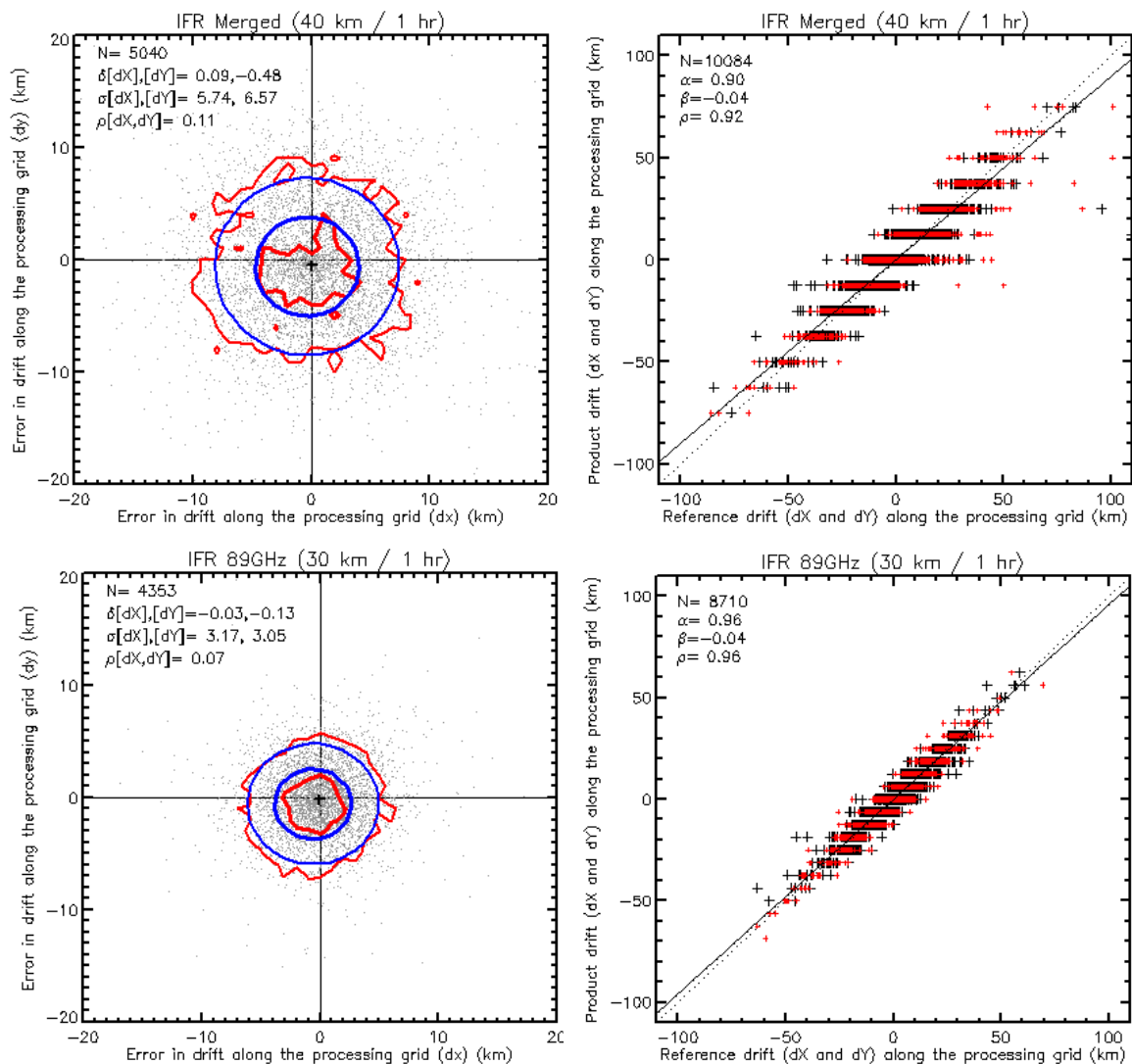
Fig. 3. (left) 2D histogram plot along dX versus dY, and (right) scatter plot of product versus reference dX (black) and dY (red) for two IFREMER products. In 2D histogram plots, red irregular contour line indicates the probability density at 68% (thick) and 95% (thin) of the sample, and blue circular contour line for corresponding the Normal distribution. The thick cross at the center indicate the bias of dX and dY. In the scatter plot, α and β are slope and intercept of linear regression (solid line), and ρ is the correctional coefficient. N is the total number counts of the validation pairs.
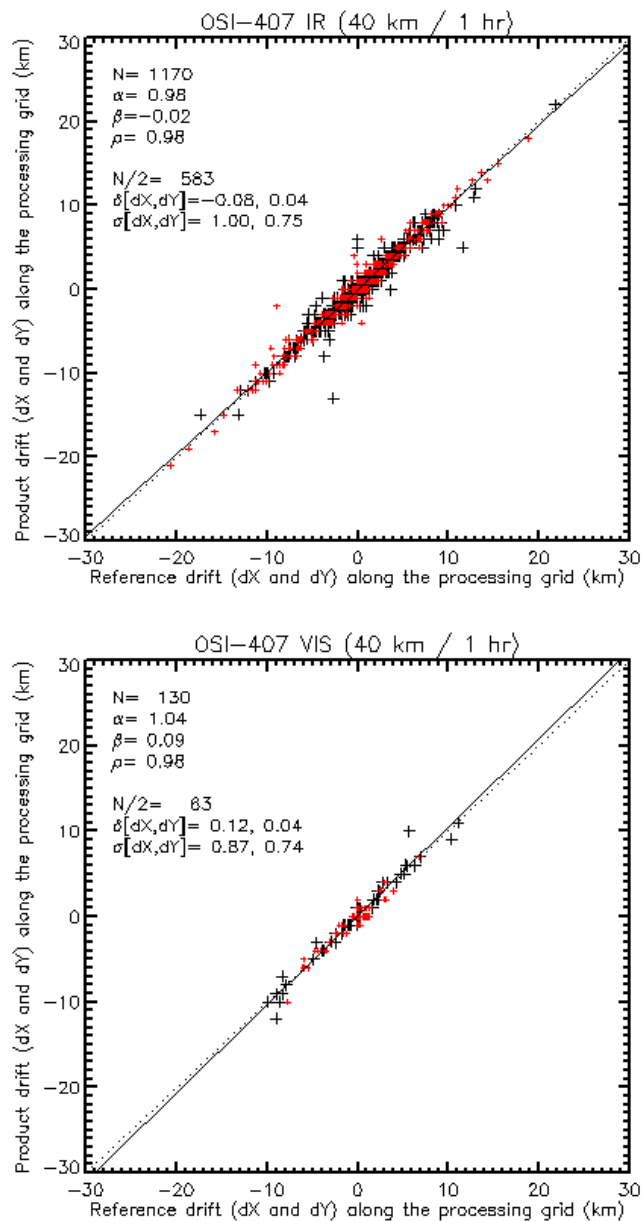
Fig. 4. Scatter plot of product versus reference dX (black) and dY (red) for OSI-407 products. α and β are slope and intercept of linear regression (solid line), and ρ is the correlation coefficient. N is the total number counts of the validation pairs.
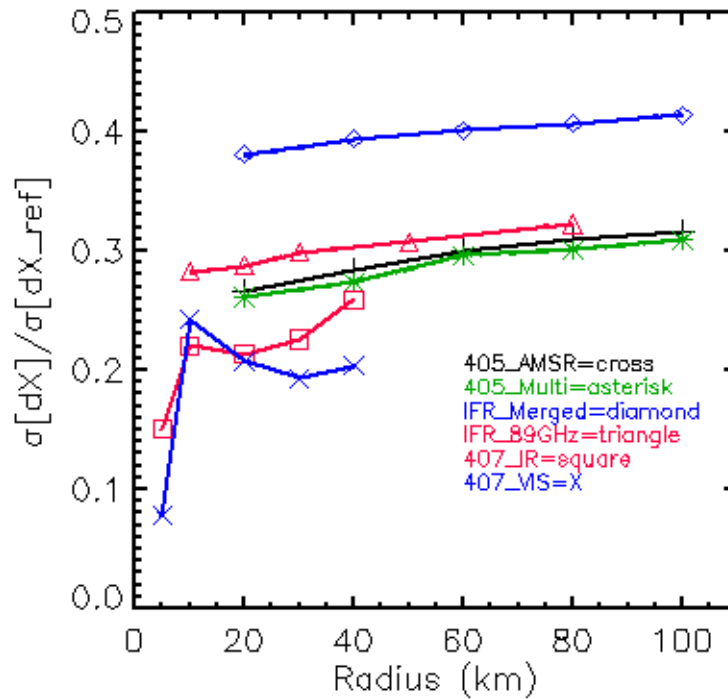
Fig. 5 Standard deviations of the error in dX (σ [dX]) normalized by standard deviation of X component of ITP trajectories (σ [dX_ref]). The latter stands for the natural variability of the 1-day, 2-day or 3-day sea ice motion as recorded by the ITPs.

5. Conclusions and Discussions

In the present study, OSI-SAF Low (405, AMSRE and Multi) and Medium (407) resolution as well as IFREMER/Cersat sea ice drift products have been validated against ITP GPS trajectories. The collocation between products and reference datasets has been made by applying "nearest-neighbor" approach, e.g. for each product grid the nearest reference ITP point in time (and space) was selected if it meets the prescribed constraints. A set of time/radius constraints was used to set up the maximum boundary within which the nearest point could be found.

A sensitivity study was conducted by applying various time/radius constraints, in order to test the variability of error statistics with different time/radius constraints. The results showed time constraints had very little effects on number counts and error statistics. While different radius constraints showed some effects on number counts and error statistics, those remained relatively stable over a range of radius constraints. Based on this results, we selected a set of time/radius constraints for further indirect comparison of the selected sea ice drift products.

Based on validation against ITP datasets, OSI-407 (Medium resolution) products showed the best error statistics. The stand-out of OSI-407 can be attributed to better ice drift tracking associated with high-resolution AVHRR images, as well as simply to less natural variability in actual ice drift associated with short time interval (i.e. less than 1 day). In fact the relative difference in error statistics between OSI-407 and OSI-405 becomes smaller when it is normalized by the variability of natural drift (Figure 5). Among the low resolution products, OSI-405 AMSR showed the best results. The difference between OSI-405 and IFR-Merged is mainly explained by the difference in time-interval, namely 2-day against 3-day. It is difficult to link this difference to any conclusion on the better accuracy of one product over the other. Although they use very similar input data (12.5 km resolution images), the OSI-405 and IFR-Merged products use different motion tracking methods. A quantization noise is clearly identified for IFR-Merged product, which is not present for OSI-405 products, that benefit from the CMCC method. After normalization by natural variability of in situ drift, the relative difference between these two becomes smaller (about 50%). IFR-89GHz, which is a 2-day drift product, shows similar validation statistics than OSI-405 AMSR, although the latter does only process the 37 GHz H&V channels (~12.5 km resolution) and not the 89 GHz channels (whose resolution is twice better).

Results from the present study generally confirm that sea ice motion can effectively be monitored from processing of pairs of satellite images. It seems that sea ice drift products using higher resolution images or/and with CMCC method yield better error statistics than the ones using lower resolution images or/and with MCC method. However, caution should be taken with any inter-comparison as these products come with both different time and spatial resolution. The natural variability of ice motion is increased for longer time period and directly impact the error statistics we report. More extended validation exercise (including more validation datasets and more products) would be required to conclude this matter in a more robust way. In particular, it would be valuable that further validation exercise include ASAR ice drift product developed by DTU that come in both 1-day and 3-day intervals, at high spatial resolution (10 km grid). In order to better understand the role of the quantization noise, a future study would also benefit from comparing 2-day drift obtained using the MCC and CMCC methods from the same satellite images, similar to what is described in [11].

6. References

[1] IFREMER ftp: ftp://ftp.ifremer.fr/ifremer/cersat/products/gridded/psi-drift/data/arctic/

[2] Lavergne, T. and S. Eastwood (2010, March). Low resolution sea ice drift Product User's Manual – v1.4. Technical Report SAF/OSI/CDOP/met.no/TEC/MA/128, EUMETSAT OSI SAF – Ocean and Sea Ice Satellite Application Facility.

[3] Girard-Ardhuin, F., R. Ezraty, D. Croizé-Fillon, and J.-F Piollé (2008, April). Sea Ice Drift in The Central Arctic Combining QuikSCAT and SSM/I Sea Ice Drift Data – User's Manual v3.0, CERSAT, IFREMER, France.

[4] Ezraty, R., F. Girard-Ardhuin, and J.-F.Piollé (2007, February). Sea Ice Drift in The Central Arctic Using The 89 GHz Brightness Temperatures of The Advanced Microwave Scanning Radiometer – User's Manual v2.0, CERSAT, IFREMER, France.

[5] Dybkjaer, G. (2009, July). Medium Resolution Sea Ice Drift Proudct User Manual - v1.0, EUMETSAT OSI SAF - Ocean and Sea Ice Satellite Application Facility.

[6] Ezraty, R., F. Girard-Ardhuin, and J.-F.Piollé (2007, February). Sea Ice Drift in The Central Arctic Estimated From SEAWINDS/QuikSCAT Backscatter Maps – v2.2, CERSAT, IFREMER, France.

[7] Met.no (2010, October). D1.2-03f – Validation at Arctic scale of low-resolved multisensor ice drift product, a report prepared for DAMOCLES - Developing Arctic Modelling and Observing Capabilities for Long-term Environment Studies.

[8] Lavergne, T. (2010 March). Validation and Monitoring of the OSI SAF Low Resolution Sea Ice Drift Product – v2.0 Technical Report SAF/OSI/CDOP/Met.no/T&V/RP/131, EUMETSAT OSI SAF – Ocean and Sea Ice Satellite Application Facility.

[9] Dybkjaer, G. (2009, December). Validation and Monitoring Document for OSI SAF Medium Resolution Sea Ice Drift Product – v0.0, EUMETSAT OSI SAF - Ocean and Sea Ice Satellite Application Facility.

[10] Stoffelen, A. (1998). Toward the true near-surface wind speed: Error modeling and calibration using triple collocation. J. Geophys. Res. 103(C4), 7755-7766.

[11] Lavergne, T., Eastwood, S., Teffah, Z., Schyberg, H., and Breivik, L.-A.. Sea ice motion from low resolution satellite sensors: an alternative method and its validation in the Arctic. *J. Geophys. Res.*, doi:10.1029/2009JC005958, *in press*, 2010.

APPENDIX A: Collection software

IDL v7.0.0 (© 2007 ITT Visual Information Solutions) was used throughout all the collocation procedure and plotting the graphs (http://www.ittvis.com/). IDL sub-routines were coded by the VS to read directly from raw data format of each product and ITP data. The main IDL code reads the all necessary sub-routines required.

Collocation was operated as follows;

• the main collocation program (e.g. colloc_os405_amsr_w_itp_all_wi_100km_3hr_v00.pro) reads the list of ITP files and loads all ITP info (via get_all_itpdata_files.pro),

• loop through ITP files and load products info of the same year, month and day (via e.g. colloc_os405_amsr_w_itp_all_wi_100km_3hr_v00.pro),

• if the time matches (i.e. the same day), calculate the time difference (t0_time_d) and get all the matching pairs within the time constraint (e.g. t0_time_d < Time_Limit),

• among the matching pairs get the point with minimum time difference,

• and if the great circle distance between the ITP point and the product grid is smaller than radius constraint, find ITP point at the end point (t1) which is closest to the product time at t1,

• if the time difference at t1 is smaller than the time constraint, print the outputs.

The outputs of main collocation program contain multiple ITP points for a product grid (i.e. not a single nearest-neighbor). Another program is required to extract the single, nearest ITP point for each product grid (find_nearest_v00.pro), and write the nearest matching pairs. This matching pairs loads into the IDL code (error_statistics_plot.pro) to calculate the error statistics and plot graphs.

Note that I used IFREMER ASCII files (not NetCDF files) and the lat/lon info at the starting and end points in the file for the calculation.

Map projection utility:

Note all the calculation was made using GCTP Projection package embedded in IDL 7.0.0.

List of IDL codes:

• colloc_os405_amsr_w_itp_all_wi_100km_3hr_v00.pro: main collocation program that catch all ITP points within 100 km radius and 3 hours for OSI-SAF 405 AMSRE product

• colloc_os405_multi_w_itp_all_wi_100km_3hr_v00.pro: main collocation program that catch all ITP points within 100 km radius and 3 hours for OSI-SAF 405 Multi (SSM/I+AMSRE+ASCAT) product

• colloc_os407_ch002_w_itp_all_wi_100km_3hr_v00.pro: main collocation program that catch all ITP points within 100 km radius and 3 hours for OSI-SAF 407 Visible (AVHRR band 2) product

• colloc_os407_ch004_w_itp_all_wi_100km_3hr_v00.pro: main collocation program that catch all ITP points within 100 km radius and 3 hours for OSI-SAF 407 IR (AVHRR band 4) product

• colloc_IFR_89GHz_w_itp_all_wi_100km_3hr_v00.pro: main collocation program that catch all ITP points within 100 km radius and 3 hours for IFREMER/Cersat AMSRE 89 GHz product

• colloc_IFR_merged_w_itp_all_wi_100km_3hr_v00.pro: main collocation program that catch all ITP points within 100 km radius and 3 hours for IFREMER/Cersat Merged (SSM/I+QuiSCAT) product

• find_nearest_v00.pro: read the output from main collocation program, find the single nearest ITP points for each product grid, and write the nearest matching pairs for given time/radius constraints

• error_statistics_plot(_OS407).pro: read the nearest matching pairs from find_nearest_v00.pro, and calculate error statistics and plot graphs

sub-routines:

• read_itpdata_file.pro: read single ITP data file

• get_all_itpdata_files.pro: load all ITP info (outputs: ref_JD, ref_lon, ref_lat, ref_ln)

• get_osi_saf_405_amsre.pro: load OSI-SAF 405 AMSRE product info (inputs: year, month and day; outputs: prd_JD, prd_lon, prd_lat)

• get_osi_saf_405_multi.pro: load OSI-SAF 405 Multi product info (inputs: year, month and day; outputs: prd_JD, prd_lon, prd_lat)

• get_osi_saf_407_vis.pro: load OSI-SAF 407 VIS (band 2) product info (inputs: year, month and day; outputs: prd_JD, prd_lon, prd_lat)

• get_osi_saf_407_ir.pro: load OSI-SAF 407 IR (band 4) product info (inputs: year, month and day; outputs: prd_JD, prd_lon, prd_lat)

• get_ifremer_89_ascii.pro: load IFREMER AMSRE 89 GHz (ASCII) product info (inputs: year, month and day; outputs: prd_JD, prd_lon, prd_lat)

• get_ifremer_mer_ascii.pro: load IFREMER Merged (ASCII) product info (inputs: year, month and day; outputs: prd_JD, prd_lon, prd_lat)